Online ISSN 1848-3380, Print ISSN 0005-1144
ATKAFF 55(3), 343–350(2014)

Lan Ma, Dongjie Bi, Houjun Wang

Analog Circuit Fault Detection Using Relative Amplitude and Relative Phase Analysis

DOI 10.7305/automatika.2014.12.605
UDK 621.317.1: 004.42; 621.38
IFAC 4.5; 4.0.3

Original scientific paper

A new method for detection of parametric faults occurring in analog circuits based on relative amplitude and relative phase analysis of the Circuit Under Test (CUT) is proposed. The relative amplitude is the common power change of the signals and the relative phase presents the relative phase offset of the signals. In the proposed method, the value of each component of the CUT is varied within its tolerance limit using Monte Carlo simulation. The upper and lower bounds of relative amplitude and phase of the CUT sampling series are obtained. While testing, the relative amplitude and phase value of the analog circuit are obtained. If any one of the relative amplitude and phase values exceed the bounds then the CUT is declared faulty. The effectiveness of the proposed method is validated through HSpice/MATLAB simulations of two benchmark circuits and the practical circuit test of Tow-Thomas circuit.

Key words: Relative amplitude, Relative phase, Parametric fault, Analog circuit, Fault detection

Otkrivanje pogreške u analognim sklopovima analizom relativne amplitude i faze. U ovome članku predložena je nova metoda otkrivanja parametarskih pogrešaka u analognim sklopovima temeljena na analizi relativne amplitude i faze promatranog sklopa (eng. Circuit Under Test, CUT). Relativna amplituda predstavlja zajedničku promjenu snage signala, dok relativna faza predstavlja pomak u fazi među signalima. U predloženoj metodi, koristeći Monte Carlo simulacije, vrijednost svake komponente CUT-a mijenja se unutar svojih granica tolerancije. Na taj način dobivaju se gornja i donja granica relativne amplitude i faze CUT uzoraka, dok se sama relativna amplituda i faza dobivaju tijekom testiranja. U slučaju da ijedan od tih dvaju faktora prelazi granicu, CUT se proglašava neispravnim. Učinkovitost predložene metode ispitana je pomoću HSpice/MATLAB simulacija nad dva referentna sklopa te na Tow-Thomas sklopu.

Ključne riječi: relativna amplituda, relativna faza, parametarska pogreška, analogni sklop, otkrivanje neispravnosti

1 INTRODUCTION

Fault diagnosis in analog circuits contains three key problems: fault detection, fault location and fault identification. Fault detection is the foundation of analog circuit fault diagnosis [1]. Nowadays, circuit design becomes more and more complex, and the reduction of the design and fabrication cost of modern electronic circuits makes fault detection a relatively expensive task [2]. This is mainly due to the difficulties inherent to the nature of analog circuits.

Use of Fourier transform analysis has proven to be an effective tool for stationary signal analysis and has been used in analog circuits fault detection [3]. In [3], the authors present a comparative sensitivity analysis between the wavelet transform and Fourier transform. It proves that the wavelet transform offers better approximation of a transient signal waveform than the Fourier transform for a fixed limiting frequency of the measured signal.

There are several works that discuss applications of wavelet transform to fault diagnosis [3–13]. In [4], the combination of PSD (Power Spectral Density) and wavelet decompositions achieves good results in fault detection of induction machines. References [9–11] apply neural networks to fault diagnosis of linear and nonlinear analog circuits. In order to preprocess the input signals, wavelet decomposition is utilized to reduce the number of inputs to the neural network and minimize the training set. In [13], a fault detection method for parametric and catastrophic faults in analog and mixed-signal circuits are given based on the wavelet analysis. Two fault detection methods are introduced, each one utilizing a different test metric which relies on wavelet energy computation.

There are two classes of wavelet transforms: continuous wavelet transforms (CWT) and discrete wavelet transforms (DWT). References [4–13] use DWT as preprocessors to extract useful information from the original signals, and employ the wavelet energy values of the measured signal as fault signatures. DWT provides a fast, local, sparse, multi-resolution analysis way to analysis signals. However, DWT also brings three main disadvantages: shift sensitivity [14], poor directionality [15], and lack of phase information. Because we are interested in extracting fault signatures from wavelet energy and wavelet phase, respectively, CWT is more suitable and we discuss only CWT in this paper. Meanwhile, complex cross wavelet transform is used in this paper in order to extract phase information from the series. Complex cross-wavelet transform exposes the relative amplitude and the relative phase of the two time series in time-frequency space. Because the relative amplitude and the relative phase of the time series depend upon the circuit parameters, they can be used as fault signatures in fault detection of analog circuits.

In this paper, a fault detection method for analog circuit parametric faults is presented based on the complex cross-wavelet analysis of the measured signal waveform, that is the output voltage (VOUT). The remainder parts of this paper are organized as follows. Section 2 outlines the fundamental theory about complex cross-wavelet transform, then discusses the choice of the mother wavelet and the method used to extracted useful information from the original series. Section 3 presents the detection method based on relative amplitude and relative phase analysis. Simulation results of the detection algorithms for two benchmark circuits and practical test results for Tow-Thomas circuit are given in Section 4. Section 5 concludes the proposed fault detection method.

2 FUNDAMENTAL THEORY

2.1 Complex Continuous Wavelet Transform

The complex continuous wavelet transform (CWT) of a time series $X(n)$ is defined as the convolution of X_n and $\varphi(t)$ [16], where $*$ indicates the complex conjugate and Δt presents the sampling interval. s is the wavelet scale and n provides the time variation. The analyzing function $\varphi(t)$ must be a complex mother wavelet and localized both in time and in frequency space.

$$W_n^X(s) = \sum_{m=1}^{N} X_m \sqrt{\frac{\Delta t}{s}} \varphi^* \left(\frac{(m-n)\Delta t}{s} \right) \quad (1)$$

Complex cross-wavelet transform of two time series X and Y is defined as:

$$W_n^{XY}(s) = W_n^X(s)\, W_n^Y(s)^* \quad (2)$$

The relative amplitude $\left| W_n^{XY}(s) \right|$ can be interpreted as the common power at the certain wavelet scale s and time variation n of the signal X and Y. The relative phase $arg\left(W_n^{XY}(s)\right)$ can be considered to be the local relative phase between X and Y in time-frequency space. Here, local relative phase means the time delay between the signals. Parametric faults of analog circuit often manifest as the common output energy variation or relative output phase offset between the faulty series and nominal series sampled from the CUT [1, 13, 17].

2.2 Choices of Complex Mother Wavelet

The proper choice of the mother wavelet plays a crucial role in the signal preprocessing. For the choice of the mother wavelet, several conditions must be satisfied. First, the mother wavelet is usually required to have a zero mean and to be localized in both time and frequency space. Second, in order to collect the relative amplitude and the relative phase information from the signal, the mother wavelet must be continuous and complex. In this paper, we focus on two different mother wavelets, namely the Morlet and Paul wavelets which are fully analyzed in paper [18].

The Morlet and Paul wavelets in the time domain are respectively shown below, where ω_0 is the frequency and m is the order:

$$Morlet : \varphi(t) = \pi^{-1/4} e^{i\omega_0 t} e^{-t^2/2} \quad (3)$$

$$Paul : \varphi(t) = \frac{2^m i^m m!}{\sqrt{\pi(2m)!}} (1 - it)^{-(m+1)} \quad (4)$$

In this paper, we will let ω_0 equal to be six in the Morlet wavelet and m equal to be four in the Paul wavelet as suggested [18].

In CWT, Fourier frequency f and wavelet scale s are not direct reciprocals of each other. In order to estimate equivalent Fourier frequency, the equations are summarized as the follow:

$$Morlet : \frac{1}{f} = \frac{4\pi s}{\omega_0 + \sqrt{2 + \omega_0^2}} \quad (5)$$

$$Paul : \frac{1}{f} = \frac{4\pi s}{2m + 1} \quad (6)$$

Another thing to be noted is that the wavelet scale s need cover this equivalent Fourier frequency, which is helpful to extract the useful information from the original series.

2.3 Information Extraction Method

In this paper, we present a method to extract sensitive relative amplitude and phase information. In analog circuit fault diagnosis, the circuit outputs are often band-limited

signals with range called F. According to equation (5) and (6), we can obtain the corresponding wavelet scales SF to the range F. $W_n^{F-N}(s)$ is expressed as the relative amplitude and phase value of the fault series to the normal series in different wavelet scale s and time variation n. We can define first-order signature extraction (SE) function as follows:

$$SE(W_n^{F-N}(s)) = W_n^{F-N}(s)|_{s=SF} \tag{7}$$

The Cone of Influence (COI) is the region of the CWT in which edge effects become important and is defined as the e-folding time for the autocorrelation of wavelet power at each scale [18]. The e-folding time ensures that the wavelet power for the discontinuity at the edge drops by a factor e^{-2} and the edge effects can be ignored. In order to overcome the edge effects of the complex cross-wavelet transform, we only calculate the relative amplitude and phase value over the significant regions which are outside the COI. The final-order signature extraction function (SEF) can be defined as follows:

$$SEF(W_n^{F-N}(s)) = SE(W_n^{F-N}(s))|_{Outside->COI} \tag{8}$$

3 PROPOSED FAULT DETECTION PROCEDURE

The fault detection procedure is implemented in two stages namely pre-testing (fault dictionary construction) stage and fault detection stage.

3.1 Pre-testing Stage

The bound limits of relative amplitude and the relative phase associated with each component are obtained using Monte Carlo simulation [19]. In the fault-free circuit, the components are allowed to vary up to 1 sigma (σ) with σ being the standard deviation from the nominal value.

Step1: Simulate the CUT in HSPICE. All components of the circuit are set to be nominal values. The circuit output is defined as X_N. And this series is used as the standard of complex cross-wavelet transform. Step2: Circuit component parameters are set to a Gaussian distribution with a variation of 1 sigma. Monte-Carlo simulation is performed M times. $X_M(i)$ represents the output of the $i-th$ Monte-Carlo simulation. Step3: Apply complex cross-wavelet transform to X_N and $X_M(i)$ series.

$$W_n^{N-N}(s) = W_n^N(s)\, W_n^N(s)^* \tag{9}$$

$$W_n^{M(i)-N}(s) = W_n^{M(i)}(s)\, W_n^N(s)^* \tag{10}$$

Step4: Use the information extraction method discussed to achieve the sensitive information.

$$AMP_{ref} = SEF(\left| W_n^{N-N}(s)\right|) \tag{11}$$

$$ARG_{ref} = SEF(arg(W_n^{N-N}(s))) \tag{12}$$

$$AMP_{mon}(i) = SEF(\left| W_n^{M(i)-N}(s)\right|) \tag{13}$$

$$ARG_{mon}(i) = SEF(arg(W_n^{M(i)-N}(s))) \tag{14}$$

Step5: Normalized variables are shown as below.

$$AMP_{REF}(i) = sig(\sum_{i=1}^{M}(AMP_{mon}(i) - AMP_{ref})) (\sum_{i=1}^{M}(AMP_{mon}(i) - AMP_{ref})^2 \frac{1}{M}) \tag{15}$$

$$ARG_{REF}(i) = sig(\sum_{i=1}^{M}(ARG_{mon}(i) - ARG_{ref})) (\sum_{i=1}^{M}(ARG_{mon}(i) - ARG_{ref})^2 \frac{1}{M}\frac{360}{2\pi}) \tag{16}$$

And

$$sig(x) = \begin{Bmatrix} 1 & x \geqslant 0 \\ -1 & x < 0 \end{Bmatrix} \tag{17}$$

The normal circuit relative amplitude response range:

$$[min(AMP_{REF})..max(AMP_{REF})] \tag{18}$$

The normal circuit relative phase response range:

$$[min(ARG_{REF})..max(ARG_{REF})] \tag{19}$$

3.2 Fault Detection Stage

Step1: Some of the single and multiple parametric faults are injected into the circuit and obtain corresponding fault series $X_F(i)$. The details are described as follow:

for each fault circuit $i = 1, \ldots, n$ do begin

$$W_n^{F(i)-N}(s) = W_n^{F(i)}(s)\, W_n^N(s)^* \tag{20}$$

$$AMP_{fault}(i) = SEF(\left| W_n^{F(i)-N}(s)\right|) \tag{21}$$

$$ARG_{fault}(i) = SEF(arg(W_n^{F(i)-N}(s))) \tag{22}$$

$$AMP_{Fault}(i) = sig(\sum_{i=1}^{M}(AMP_{fault}(i) - AMP_{ref})) (\sum_{i=1}^{M}(AMP_{fault}(i) - AMP_{ref})^2 \frac{1}{M}) \tag{23}$$

$$ARG_{Fault}(i) = sig(\sum_{i=1}^{M}(ARG_{fault}(i) - ARG_{ref}))$$
$$(\sum_{i=1}^{M}(ARG_{fault}(i) - ARG_{ref})^2 \frac{1}{M}\frac{360}{2\pi}) \quad (24)$$

end

Step2:

for each fault circuit i = 1,. . . .n do begins

if $AMP_{Fault}(i) < min(AMP_{REF})$ or $AMP_{Fault}(i) > max(AMP_{REF})$ then a relative-amplitude fault occurs in the circuit.

if $ARG_{Fault}(i) < min(ARG_{REF})$ or $ARG_{Fault}(i) > max(ARG_{REF})$ then a relative-phase fault occurs in the circuit.

end

4 SIMULATION AND EXPERIMENT RESULTS

The proposed method is validated through the practical Tow-Thomas circuit and two benchmark circuits: the low-pass filter circuit and leapfrog circuit. The test algorithms in Section 3 have been implemented in MATLAB and have been utilized for testing various analog circuits.

4.1 Low-pass Filter Simulation Results

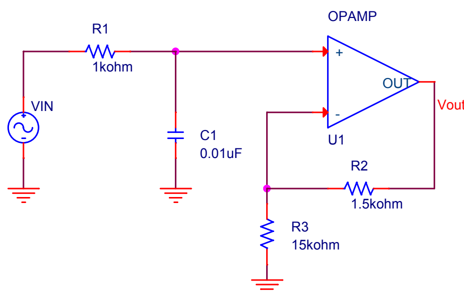

Fig. 1. Low-pass filter circuit benchmark

Low-pass filter circuit is shown in Fig. 1. A low-frequency sinusoidal input of 1kHz with an amplitude of 3V is applied to input VIN. The tolerance limits for the normal circuit are obtained from a set of 2 000 Monte-Carlo simulations. For the fault-free circuit, the VOUT is sampled at a 100KSPS (thousand samples per second) sampling rate and stored 2048 samples per waveform. The upper and lower bounds of the relative amplitude and the relative phase are obtained and showed in Table 1, where AMP(Morlet) indicates the relative amplitude value using the Morlet wavelet and ARG(Morlet) presents the relative phase value using the Morlet wavelet. Then some parametric faults are independently injected into the circuit and the relative amplitude and the relative phase values are obtained and shown in Table 2 for every fault. MorletOBS indicates an out of bound signature using the Morlet mother wavelet. C1-6Sigma fault means a '-'6 sigma variation of the value of C1.

Table 1. Bounds of relative amplitude and phase of low-pass filter

Bound of Fault Signature	Min	Max
AMP(Morlet)	-3.413713	8.058208
ARG(Morlet)	-1.476805	1.177993
AMP(PAUL)	-1.201012	2.834847
ARG (PAUL)	-1.476908	1.176682

Table 2. Test results of the proposed fault detection method applied to low-pass filter circuit

Fault Type	AMP(Morlet)	ARG(Morlet)	MorletOBS
C1-6Sigma	8.244857	1.671774	AMP/ARG
R2-6Sigma	-4.751803	0.924036	AMP
R2+6Sigma	15.116115	-0.372929	AMP
R3-6Sigma	96.080808	-0.512812	AMP
R3+6Sigma	-4.535191	0.851484	AMP
Fault Type	AMP(Paul)	ARG(Paul)	PaulOBS
C1-6Sigma	2.900995	1.669873	AMP/ARG
R2-6Sigma	-1.671385	0.923032	AMP
R2+6Sigma	5.317709	-0.372441	AMP
R3-6Sigma	33.801105	-0.512178	AMP
R3+6Sigma	-1.595194	0.850570	AMP

For C1-6sigma fault, the corresponding relative amplitude and phase values are obtained in Table 2. While compared with the lower and upper bounds it can be found that the AMP and ARG parts are exceeding the bound and hence this fault is detected. The R2-6Sigma, R2+6Sigma, R3-6Sigma, R3+6Sigma faults are more sensitive to the relative amplitude analysis than the relative phase analysis.

4.2 Leapfrog Circuit Simulation Results

The leapfrog circuit shown in Fig. 2 passes signal from DC to 1.4kHz for desired system operation. The input VIN is a 1kHz sinusoidal wave with an 3V amplitude. VOUT is sampled with 100KSPS sampling rate and stored 2048 samples per waveform. The Monte-Carlo simulation is performed for 2000 times. Similarly parametric faults occurring in a Leapfrog circuit have been detected by applying the proposed method. The bound limits of its relative amplitude and phase and the results are shown in Table 3 and 4.

The upper and lower bounds of the leapfrog circuit are different with different complex mother wavelets. The

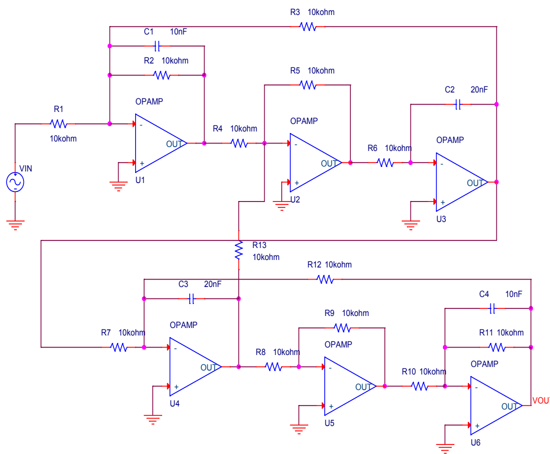

Fig. 2. Leapfrog circuit benchmark

Table 3. Bounds of relative amplitude and phase of leapfrog circuit

Bound of Fault Signature	Min	Max
AMP(Morlet)	-13.498259	12.343993
ARG(Morlet)	-8.895469	9.295972
AMP(PAUL)	-4.740685	4.336003
ARG (PAUL)	-8.885899	9.293368

ranges of the relative amplitude of the fault-free circuit change significantly. For the Morlet mother wavelet, the AMP(Morlet) absolute range is about 22.794231, while the AMP(PAUL) is about 9.076688. We can infer that the Morlet mother wavelet in the proposed method has a better resolution in relative amplitude analysis. On the contrary, the ranges of the relative phase of the fault-free circuit are almost the same. It can be contributed to the nature of the relative phase analysis.

For C1-6sigma fault, the relative amplitude value crosses the upper boundary value of 12.343993, and the parametric fault in C1 has been detected using relative amplitude analysis. For C3+6sigma fault, the relative phase value crosses the lower boundary value of -8.895469. Thereby the parametric fault in C3 has been detected using relative phase analysis. Using either Morlet or Paul mother wavelet, the C1-6Sigma and C3+6Sigma faults can be detected. The main effect of choices of mother wavelets is the resolution in distinguishing faults using either the relative amplitude analysis or the relative phase analysis.

According to the test results, it is easily seen that the signatures produced by the proposed method have the ability of preventing aliasing and high robustness. The relative amplitude and relative phase of each fault correspond to one and only one fault in the circuit under test. Plotting the relative amplitude values as x-axis and the relative phase values as y-axis, some typical parametric faults of the leapfrog circuit are demonstrated in Fig. 3. The Morlet mother wavelet is used for the following leapfrog circuit fault detection. The yellow square represents the fault-free area and any fault lying inside the square cannot be detected. C3-1Sigma-C3-40Sigma fault means that the value of C3 decreases from 1 sigma to 40 sigma, and the step of the decrease is 0.5 sigma.

Table 4. Test results of the proposed fault detection method applied to low-pass filter circuit

Fault Type	AMP(Morlet)	ARG(Morlet)	MorletOBS
C1-6Sigma	13.958415	9.011746	AMP
C3-6Sigma	15.073037	11.909609	AMP/ARG
C3+6Sigma	-13.169358	-16.475253	ARG
C4+6sigma	-8.451804	-13.481419	ARG
R2-6Sigma	-17.605256	-8.142736	AMP
R6-6sigma	8.148630	14.872265	ARG
R8+6sigma	-14.687502	-11.018723	AMP/ARG
R11+6sigma	-14.032108	-13.088741	AMP/ARG
Fault Type	**AMP(Paul)**	**ARG(Paul)**	**PaulOBS**
C1-6Sigma	4.900607	9.008554	AMP
C3-6Sigma	5.290877	11.907371	AMP/ARG
C3+6Sigma	-4.617859	-16.460244	ARG
C4+6sigma	-2.964703	-13.469648	ARG
R2-6Sigma	-6.180655	-8.134594	AMP
R6-6sigma	2.856833	14.872338	ARG
R8+6sigma	-5.156037	-11.006162	AMP/ARG
R11+6sigma	-4.923924	-13.075026	AMP/ARG

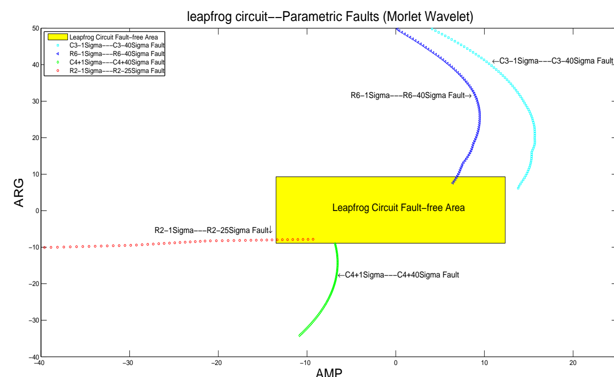

Fig. 3. Leapfrog circuit typical parametric fault

C3-5Sigma-C3-40Sigma fault can be detected using the relative phase analysis, and it shows that the sampling series of the fault circuit have a positive time delay compared with the fault-free circuit. On the contrary, there is a negative time delay between the fault circuit and fault-free circuit, when C4 value increases from 1 sigma to 40 sigma. These typical faults are sensitive to the relative phase anal-

ysis. R6-3Sigma-R6-40Sigma faults are sensitive to the relative phase analysis. Similarly, With R2 value changing from 5 Sigma to 25 Sigma, the relative amplitude value changes from -13.5 to -40. These faults show the fact that the energy of the fault circuit sampling series change significantly.

4.3 Experiments on Tow-Thomas Filter Circuit

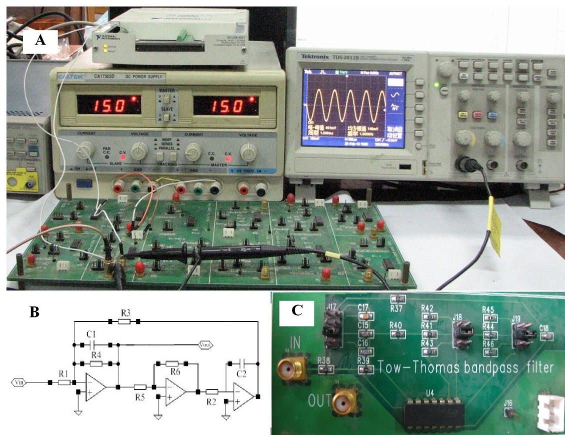

Fig. 4. (A)Test system picture (B)Schematic of Tow-Thomas filter circuit (C)Actual Tow- Thomas filter circuit

The structure and parameters of Tow-Thomas filter circuit is illustrated in Fig. 4(B) with $R_1 = R_2 = R_3 = R_4 = 16kohm$, $R_5 = R_6 = 10kohm$ and $C_1 = C_2 = 1nf$. The actual circuit is shown in Fig. 4(C), and the amplifier in the circuit is TL084 produced by TI. The actual test system is shown in Fig. 4(A). It consists of a National Instruments USB-6251 multifunction data acquisition (DAQ), which is used to generate the input sinusoidal signal and acquire the output signal. Eight fault cases are randomly chosen, and the experimental results using Morlet mother wavelet are listed in Table 5. Especially, the relative amplitude and the phase value obtained by using the proposed method also show strong robustness for actual circuit. For example, shown in Table 5, the relative amplitude and the relative phase value of the Fault No.1 which is the C_1 down drift parametric fault is different from other parametric faults. In Table 5, Fault No.1 and Fault No.2 represent two types of parametric faults of one component. The same is the case with Fault No.3 and Fault No.4, Fault No.5 and Fault No.6, respectively. Fault No.7 is a multiple parametric fault caused by the variations of the C1 and R6 and R2 together. Fault No.8 is the same case as Fault No.7.

Table 5 is an illustration of the good discrimination effects for different parametric faults in analog circuit by the proposed method. The experimental results show that the faults can be precisely located with-

Table 5. Test results of the proposed method applied to Tow-Thomas circuit using Morlet mother wavelet

Fault No.	Faulty	AMP(Morlet)	ARG(Morlet)
1	C1 variation (1nF->0.82nF)	1.494697	8.755999
2	C1 variation (1nF->1.2nF)	-1.636697	-10.153168
3	R6 variation (10k->9.1k)	1.138892	-7.348737
4	R6 variation (10k->11k)	4.440179	6.949636
5	R2 variation (16k->14.7k)	-0.561991	7.696691
6	R2 variation (16k->18k)	3.479317	-7.357379
7	Fault 1 + Fault 4 + Fault 5	-1.263060	18.214645
8	Fault 2 + Fault 3 + Fault 6	-4.099782	-18.526999
0	Fault free	Min(AMP))–Max(AMP)= [-7.000810–6.861794]; Min(ARG)–Max(ARG)= [-6.472527–6.657202];	

Table 6. Test results of the proposed method applied to Tow-Thomas circuit using Paul mother wavelet

Fault No.	Faulty	AMP(Paul)	ARG(Paul)
1	C1 variation (1nF->0.82nF)	0.523009	8.736694
2	C1 variation (1nF->1.2nF)	-0.563765	-10.132291
3	R6 variation (10k->9.1k)	0.397835	-7.353568
4	R6 variation (10k->11k)	1.560994	6.964533
5	R2 variation (16k->14.7k)	-0.207224	7.670346
6	R2 variation (16k->18k)	1.233490	-7.343457
7	Fault 1 + Fault 4 + Fault 5	-0.450518	18.204644
8	Fault 2 + Fault 3 + Fault 6	-1.448169	-18.512438
0	Fault free	Min(AMP))–Max(AMP)= [-2.457858—2.430449]; Min(ARG)–Max(ARG)= [-6.485154— 6.654602];	

out aliasing. For example, for Fault No.5, the experimental AMP/ARG is $[-0.561991, 7.696691]$, whereas AMP/ARG is $[1.494697, 8.755999]$ for Fault No.1. They are different and all of them are beyond the nominal range of the fault-free circuit, so Fault No.1 and Fault No.5 can easily be separated. The same conclusion can be drawn for any other cases as well. Furthermore, the

multiple parametric faults can also be detected by using the proposed method. For example, AMP/ARG is $[-1.263060, 18.214645]$ for Fault No.7 and experimental AMP/ARG is $[-4.099782, -18.526999]$ for Fault No.8. They are quite different, so two multiple parametric faults can be detected respectively.

The experimental results of the proposed method are listed in Table 6 when the mother wavelet is Paul mother wavelet. The experimental results show that the proposed method shares the high efficiency of diagnosis for the same fault by either the Morlet or the PAUL mother wavelet. Because the relative phase values of the same fault are almost identical using the two mother wavelet, we can infer that the choice of different mother wavelets does little affect on the relative phase analysis of the proposed method. On the contrary, the relative amplitude analysis using the Morlet mother wavelet has a higher fault resolution than using the PAUL mother wavelet.

5 CONCLUSION

In this paper, the complex cross-wavelet transform of the measured output voltage VOUT for analog circuit test has been studied, and we propose a new parametric faults detection method, which extracts fault signatures not only from the wavelet energy values of the measured signal, but also the wavelet phase values. The relative amplitude and the relative phase analysis proposed in this paper can detect parametric faults occurring in analog circuits efficiently. Tests results confirm that fault detection of analog circuits is fairly easy with the combination of the relative amplitude and relative phase analysis. Two benchmark circuits and Tow-Thomas filter circuit have been investigated to validate the proposed method.

REFERENCES

[1] J. W. Bandler and A. E. Salamai, “Fault diagnosis of analog circuits,” *Proceedings of the IEEE*, vol. 73, no. 8, pp. 1279–1325, 1985.

[2] G. Damian and J. Rutkowski, “Fault diagnosis of analog circuits - the svm approach,” *Metrology and Measurement System*, vol. 13, no. 4, pp. 583–598, 2009.

[3] S. Bhunia and K. Roy, “A novel wavelet transform-based transient current analysis for fault detection and localization,” *IEEE Transactions on Very Large Scale Integration (VLSI) Systems*, vol. 13, no. 4, pp. 503–507, 2005.

[4] J. O. J. Cusido, L. Romeral and J. Rosero, “Fault detection in induction machines using power spectral density in wavelet decomposition,” *IEEE Transactions on Industrial Electronics*, vol. 55, no. 2, pp. 633–643, 2008.

[5] J. Q. Zhang and Y. Yan, “A wavelet-based approach to abrupt fault detection and diagnosis in sensors,” *IEEE Transactions on Industrial Electronics*, vol. 53, no. 2, pp. 431–436, 2001.

[6] L. Eren and M. J. Davaney, “Bearing damage detection via wavelet packet decomposition of the stator current,” *IEEE Transactions on Instrumentation and Measurement*, vol. 53, no. 2, pp. 431–436, 2004.

[7] H. H. S. H. Kia and G. Capolino, “Diagnosis of broken bar fault in induction machines using discrete wavelet transform without slip estimation,” *IEEE Transactions on Industry Applications*, vol. 45, no. 4, pp. 1395–1404, 2009.

[8] D. K. P. M. G. Dimopoulos, A. D. Spyronasios and A. A. Hatzopoulos, “Wavelet energy-based testing using supply current measurements,” *IET Science, Measurement and Technology*, vol. 4, no. 2, pp. 76–85, 2010.

[9] M. Aminian and F. Aminian, “A modular fault-diagnostic system for analog electronic circuits using neural networks with wavelet transform as a preprocessor,” *IEEE Transactions on Instrumentation and Measurement*, vol. 56, no. 5, pp. 1546–1554, 2007.

[10] M. Aminian and F. Aminian, “Neural-network based analog-circuit fault diagnosis using wavelet transform as preprocessor,” *IEEE Transactions on Circuits System II*, vol. 47, no. 2, pp. 151–156, 2000.

[11] F. Aminian and M. Aminian, “Fault diagnosis of nonlinear circuits using neural networks with wavelet and fourier transforms as preprocessors,” *Journal of Electronic Testing*, vol. 17, no. 1, pp. 471–481, 2001.

[12] V. Stopjakova, “Defect detection in analog and mixed circuits by neural networks using wavelet analysis,” *IEEE Transactions on Reliability*, vol. 54, no. 3, pp. 441–448, 2005.

[13] M. G. D. A. D. Spyronasios and A. A. Hatzopoulos, “Wavelet analysis for the detection of parametric and catastrophic faults in mixed-signal circuits,” *IEEE Transactions on Instrumentation and Measurement*, vol. 60, no. 6, pp. 2025–2038, 2011.

[14] G. Strang, “Wavelets and dilation equations: a brief introduction,” *Society for Industrial and Applied Mathematics Review.*, vol. 31, no. 4, pp. 614–627, 1989.

[15] D. T. Burns, S.Rogers and M.Oxley, “Discrete, spatiotemporal, wavelet multiresolution analysis method for computing optical flow,” *Optical Engineering*, vol. 33, no. 7, pp. 2236–2247, 1994.

[16] I. C. Daubechies, *Ten lectures on wavelets*. Philadelphia: CBMS-NSF Regional Conference Series in Applied Mathematics, 1992.

[17] J. Savir and Z. Guo, “Test limitations of parametric faults in analog circuits,” *IEEE Transactions on Instrumentation and Measurement*, vol. 52, no. 5, pp. 1444–1454, 2003.

[18] C.Torrence and G. P.Compo, “A practical guide to wavelet analysis,” *Bulletin of the American Meteorogical Society*, vol. 79, no. 1, pp. 61–78, 1998.

[19] K. M. R.Kondagunturi, E. Bradley and C. Stroud, “Benchmark circuits for analog and mixed-signal testing,” in *Proceedings of the IEEE Southeastcon Conference*, (Lexington), pp. 217–220, Mar 1999.

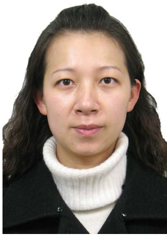

Lan Ma received the B.S., M.S degrees from the University of Electronic Science and Technology of China (UESTC), Chengdu, China, in 2002 and 2007 respectively. She is currently working toward the Ph.D. degree in technology and instruments for measurement and test in the School of Automation, UESTC. Her research interests include fault diagnosis and fault identification of analog circuits.

Dongjie Bi received the B.S., M.S degrees from the University of Electronic Science and Technology of China (UESTC),Chengdu, China, in 2009 and 2011 respectively. He is currently working toward the Ph.D. degree in measuring and testing technology and instruments in the School of Automation Engineering. His research interests include fault diagnosis and fault identification of analog circuits.

Houjun Wang received the M.S. degree in measuring and testing technology and instruments and the Ph.D. degree in signal and information processing from the University of Electronic Science and Technology of China, Chengdu, China, in 1982 and 1991, respectively. He is currently a Professor of the School of Automation Engineering, University of Electronic Science and Technology of China. His research interests include signal processing, signal testing, and design for tests. Dr. Wang is a member of the National Electronic Measuring Instrument Standardization Technology Committee.

AUTHORS' ADDRESSES

Lan Ma, M.Sc.
Dongjie Bi, M.Sc.
Prof. Houjun Wang, Ph.D.
School of Automation Engineering,
University of Electronic Science and Technology of China,
No.2006, West Hi-Tech Zone, Chengdu, Sichuan, China
email: malan@uestc.edu.cn,bidongjie1985@hotmail.com, hjwang@uestc.edu.cn

Received: 2013-06-25
Accepted: 2014-03-05